

Review

Cite this article: Eisen SR, Dauphin-Ducharme P and Johnson PE (2024). Solution-based biophysical characterization of conformation change in structure-switching aptamers. *Quarterly Reviews of Biophysics*, **57**, e9, 1–14 <https://doi.org/10.1017/S0033583524000076>

Received: 20 February 2024

Revised: 29 April 2024

Accepted: 10 May 2024

Keywords:



aptamers; biophysical methods; DNA; ligand-induced folding; structural change

Corresponding author:

Philip E. Johnson;

Email: pjohnson@yorku.ca

Solution-based biophysical characterization of conformation change in structure-switching aptamers

Sophie R. Eisen¹, Philippe Dauphin-Ducharme²  and Philip E. Johnson¹ 

¹Department of Chemistry, York University, Toronto, ON, Canada and ²Département de chimie, Université de Sherbrooke, Sherbrooke, QC, Canada

Abstract

Structure-switching aptamers have become ubiquitous in several applications, notably in analytical devices such as biosensors, due to their ease of supporting strong signaling. Aside from their ability to bind specifically with their respective target, this class of aptamers also undergoes a conformational rearrangement upon target recognition. While several well-studied and early-developed aptamers (e.g., cocaine, ATP, and thrombin) have been found to have this structure-switching property, the vast majority do not. As a result, it is common to try to engineer aptamers into switches. This proves challenging in part because of the difficulty in obtaining structural and functional information about aptamers. In response, we review various readily available biophysical characterization tools that are capable of assessing structure switching of aptamers. In doing so, we delve into the fundamentals of these different techniques and detail how they have been utilized in characterizing structure-switching aptamers. While each of these biophysical techniques alone has utility, their real power to demonstrate the occurrence of structural change with ligand binding is when multiple techniques are used. We hope that through a deeper understanding of these techniques, researchers will be better able to acquire biophysical information about their aptamer–ligand systems and accelerate the translation of aptamers into biosensors.

Table of contents

Introduction	1
Structure-switching aptamers	2
Structural and binding methods to assess structure-switching in aptamers	3
Nuclear magnetic resonance spectroscopy	3
Isothermal titration calorimetry	5
Circular dichroism spectroscopy	6
Thermal melt analysis	6
Small-angle X-ray scattering	7
Native ion mobility-mass spectrometry	8
Fluorescence-based methods	8
Fluorescence quenching and FRET-based aptamer beacon sensors	8
Fluorescent aptamer sensors using complementary displacement strand	9
Split aptamer fluorescent and FRET-based sensors	10
Conclusions	11

Introduction

Aptamers are short, single-stranded nucleic acids that are selected to bind molecular targets, including small molecules, proteins, and cells. They are produced via an *in vitro* evolutionary process coined systematic evolution of ligands by exponential enrichment (SELEX; DeRosa *et al.*, 2023). Using SELEX, aptamers have been produced to bind their target, often with high specificity and affinity. Similar to their naturally occurring counterparts, riboswitches, some aptamers derived from SELEX can have an additional function: an ability to undergo a binding-induced conformational change (Nutiu and Li, 2005; Morse, 2007; Oh *et al.*, 2010; Yang *et al.*, 2016).

Structure-switching aptamers are advantageous for the development of biosensors. Their ability to undergo a binding-induced conformational rearrangement can be easily transduced into measurable optical or electrochemical signals (Lau and Li, 2014). Analogous to receptors found in nature, this class of aptamers can support signaling that is inherently independent of surface fouling, a process detrimental to the long-term stability of biosensors. Additionally, target

© The Author(s), 2024. Published by Cambridge University Press. This is an Open Access article, distributed under the terms of the Creative Commons Attribution licence (<http://creativecommons.org/licenses/by/4.0>), which permits unrestricted re-use, distribution and reproduction, provided the original article is properly cited.

binding kinetics (on and off rates) to these aptamers is relatively fast, especially in the case of small molecules. As a result, structure-switching aptamers help support continuous, real-time, and rapid (<5 min) measurements of clinically relevant targets (drugs, steroids, chemotherapeutics, antibiotics, etc.) directly in undiluted complex matrices, such as whole blood and even in the body for prolonged periods (Kwon *et al.*, 2020; Cánovas *et al.*, 2022; Xie *et al.*, 2022; Alkhamis *et al.*, 2024). These unprecedented capabilities are thus paving the way toward the development of point-of-care diagnostic tools to solve the paradigm of personalized medicine.

Considering the importance of structure-switching aptamers in such applications, we first look at aptamers that have been discovered to inherently undergo a conformational change upon ligand binding and review the secondary and tertiary structure motifs they adopt. Since many aptamers must be engineered post-SELEX to possess a structure-switching function, we look at biophysical methods, structural, binding, and fluorescent techniques, capable of determining that structural changes occur when aptamers bind their target.

Structure-switching aptamers

For the purpose of this review, we define structure-switching aptamers as nucleic acid sequences that undergo a structural change with target binding. This may be from a structured free state to a differently structured bound state or ones that undergo binding-induced folding. In the latter case, an aptamer goes from a free state to a bound state that is less dynamic or where more of the nucleotides are in a region of defined secondary structure. The structural changes incurred by aptamers can thus be of various scales. For instance, the MN4 cocaine-binding aptamer already adopts a structure in the free state and undergoes small conformational rearrangements with target binding that create 1–2 new base pair interactions. Ultimately, this does not alter the tertiary structure of the aptamer. The MN19 cocaine-binding aptamer, in contrast, transitions from an unstructured or dynamic free state and undergoes a large structural change in which a new stem (stem 1) forms (Cekan *et al.*, 2009; Neves *et al.*, 2010).

There are a variety of secondary structural changes that aptamers can undergo with ligand-induced folding. A first and well-

studied case is of aptamers that form a three-way junction due to target binding (Figure 1a). Examples of this are the MN19 cocaine-binding aptamer and the related MS2 steroid-binding aptamers. These aptamers contain a loosely folded stem in the free state, which upon binding their target transition to three-way junction conformations (Reinstein *et al.*, 2011, 2013; Neves *et al.*, 2017). A second well-studied case is where ligand-binding triggers folding of the aptamer into a G-quadruplex (Figure 1b). The 15-nucleotide thrombin-binding (Li *et al.*, 2002; Lin *et al.*, 2011), serotonin-binding and ochratoxin A-binding aptamers (Yang *et al.*, 2011; Nakatsuka *et al.*, 2018; Xu *et al.*, 2022) are examples of this where they transition from an unfolded free state to a G-quadruplex structure. A third common case is when an internal loop of the aptamer becomes more structured (Figure 1c). The 27-nucleotide ATP-binding, the caffeine-binding and glucose-binding DNA aptamers (Nakatsuka *et al.*, 2018; Huang and Liu, 2022; Lu *et al.*, 2022) are examples of a system in which a stem with a large asymmetrical internal loop is found in the free state. For the ATP-binding DNA aptamer, the internal loop becomes more ordered as additional base pairs form when the aptamer binds its ligand (Lin and Patel, 1997).

While several aptamers have been discovered to inherently undergo a conformational change upon ligand binding, such as the ATP-binding DNA aptamer (Lin and Patel, 1997), they more commonly must be engineered post-SELEX to possess this ability. This can be done by: (1) splitting sequences into two or more strand fragments, referred to as split-aptamers (Figure 1d), (2) hybridizing with a complementary strand, a molecular beacon approach, or (3) truncating using exonuclease digestion. Examples of developing split aptamers are numerous, and include the ATP, cocaine, codeine, and thrombin-binding aptamers. Each has been made as split aptamers in which fragments remain separate in the free state and then assemble or hybridize upon target binding to form the complete aptamer–ligand complex (Stojanovic *et al.*, 2000; Liao *et al.*, 2012; Kent *et al.*, 2013; Liu *et al.*, 2014; Bing *et al.*, 2017; Debais *et al.*, 2020). Exonuclease digestion has been developed by the Xiao group to introduce structure switching into selected aptamers by reacting the aptamer in the presence of its ligand with a DNA exonuclease to determine the structured core of the

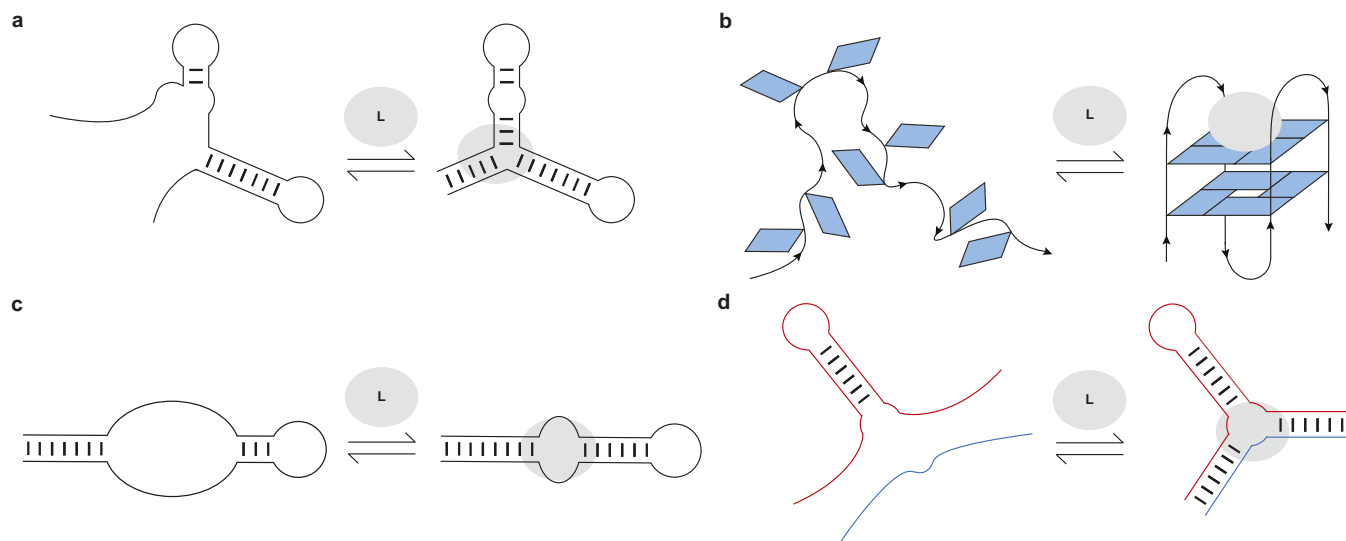


Figure 1. Different types of aptamer conformational changes induced by ligand binding. **(a)** Three-way junction formation. **(b)** G-quadruplex formation. **(c)** Reduction in internal loop size. **(d)** Assembly of split aptamer strands.

aptamer. Though useful, this technique has not yet been widely adopted (Canoura *et al.*, 2018; Wang *et al.*, 2018; Alkhamis *et al.*, 2023).

Given that many aptamers are natively unable to undergo structural rearrangement, we review analytical tools that provide such information with the hopes that this will support researchers in engineering aptamers to become structure switching.

Structural and binding methods to assess structure-switching in aptamers

Nuclear magnetic resonance spectroscopy

Nuclear magnetic resonance (NMR) spectroscopy is a solution-based technique where a sample is placed in a strong external magnetic field enabling certain nuclei in the sample to be studied. For nucleic acid aptamers, these nuclei are ^1H , ^{13}C , ^{15}N , and ^{31}P . These spin $\frac{1}{2}$ nuclei will resonate at a frequency that depends on their chemical identity and their specific local environment. ^1H nuclei are particularly easy to examine due to their high natural abundance and are rich in information about their local environment. In contrast, nuclei such as ^{13}C and ^{15}N are more difficult to work with due to their low natural abundance, though isotopically enriched DNA and RNA aptamer samples can be prepared (Zimmer and Crothers, 1995; Le *et al.*, 2015; Dayie *et al.*, 2022; Wang *et al.*, 2024). Due to the analytical capabilities offered by NMR spectroscopy, it has been used to determine the three-dimensional structures of a number of DNA and RNA aptamers, both free and ligand-bound (Sakamoto, 2017; Xu *et al.*, 2022, 2023). While determining the structure of free and bound forms of aptamers is a clear way to determine conformational change that occurs with binding, it is not necessary to determine a three-dimensional structure to discover if conformational change occurs with ligand binding.

One-dimensional (1D) ^1H NMR can provide valuable information on the structural changes of aptamers with target binding through studying the peaks of imino protons. Imino proton signals of aptamers typically arise in ^1H NMR spectra when protected from exchange with bulk water by being hydrogen bonded such as in base pairs (Sakamoto, 2017). Imino protons are located downfield between 10 and 15 ppm, which sets them apart from other proton signals in the spectra (Sakamoto, 2017). When performing a titration of an aptamer with its ligand, one obtains a series of 1D ^1H NMR spectra ranging from the free to ligand-bound aptamer. Depending on the appearance and/or disappearance of certain signals, this can provide information on the ability of the aptamer to undergo a change in structure as hydrogen-bonded nucleotides get formed or broken.

Two-dimensional (2D) NMR experiments are useful in assigning signals to particular nuclei in aptamers through their ability to interact with other nuclei. This is typically achieved using 2D Nuclear Overhauser Effect Spectroscopy (NOESY) in which the imino proton signals from ^1H NMR can be correlated to specific bases within the structure of the aptamer (Wüthrich, 1986; Lin and Patel, 1997). A detailed comparison of the free and ligand-bound imino proton spectra often yields insights into structural changes incurred by the aptamer upon ligand binding. An increase in the number of imino proton signals with ligand addition suggests that the aptamer forms new base pairs with ligand binding (Churcher *et al.*, 2020). Conversely, a decrease in the number of imino proton signals indicates that the aptamer may lose base pairs during binding. A narrowing and sharpening of imino proton peaks during

titration can demonstrate that the aptamer adopts a more well-defined structure upon ligand binding (Neves *et al.*, 2017). Overall, 1D ^1H NMR in conjunction with imino proton assignments from 2D NOESY can be used to effectively probe target-induced conformational changes of aptamers.

Neves *et al.* (2010) performed 1D ^1H NMR to monitor a titration of the three-way junction MN19 and MN4 cocaine-binding aptamers with cocaine to show that MN19 undergoes structural switching while MN4 does not. In the ^1H NMR spectra of the MN19 aptamer, the imino proton signals were broader and fewer in number in the free state compared to the cocaine-bound state (Figure 2a). With cocaine addition, the imino proton signals sharpened and new imino proton peaks corresponding to G29, G30, G31, and T32 became visible. These ^1H NMR spectral changes demonstrated that the MN19 aptamer is loosely folded in the free state and forms stem 1 of its three-way junction structure and two GA mismatches upon cocaine binding. In contrast, there was little change in the sharpness and total number of imino proton peaks of the MN4 aptamer between its free and cocaine-bound states (Figure 2b). Although the imino protons of G31 and T32 were visible for both the free and cocaine-bound MN4 aptamer, they changed chemical shift in the presence of cocaine. These peaks likely shifted position with cocaine addition due to their proximity to the cocaine-binding site of the MN4 aptamer. This ^1H NMR titration provided evidence that the MN4 aptamer is prefolded in the free state and retains its three-way junction structure when binding cocaine. Previous ^1H NMR studies involving the titration of quinine have also shown the structure-switching binding mechanism of the MN19 aptamer and the prefolded nature of the MN4 aptamer is retained (Reinstein *et al.*, 2013).

1D ^1H NMR can be used to study the ligand-induced conformational changes of aptamers with internal loops and hairpin structures. Lin and Patel (1997) performed 1D ^1H NMR to study a titration of the 27-nucleotide AMP-binding DNA aptamer with adenosine monophosphate (AMP). In the absence of AMP, broad imino proton signals were observed in the aptamer's asymmetrical internal loop. When the aptamer bound two AMP molecules, the imino proton signals of the internal loop narrowed and new imino proton signals appeared. These ^1H NMR spectral changes demonstrated that AMP binding induces the formation of six new mismatched base pairs, causing the aptamer's internal loop to decrease in size. Additionally, Robertson *et al.* (2000) used 1D ^1H NMR to monitor a titration of the argininamide-binding DNA aptamer with its target. When argininamide was added to the aptamer, new imino proton signals in the ^1H NMR spectra became visible that corresponded to bases in the loop of the aptamer's hairpin. Further analysis with NOESY data showed that argininamide binding causes three new base pairs to form in the loop and facilitates formation of the aptamer's binding pocket.

Aside from demonstrating base pair formation, 1D ^1H NMR can be used to show a decrease in the number of base pairs with ligand binding. Oguro *et al.* (2017) performed 1D ^1H NMR to study conformational changes of the SL_2 RNA spermine-binding aptamer in the presence of its target. The aptamer has a two stem-loop structure consisting of a terminal-side stem (T-Stem) and loop-side stem. With spermine addition, six imino proton signals disappeared from the ^1H NMR spectrum of the aptamer and five of these signals corresponded to bases in the T-Stem. This indicated that spermine binding by the aptamer may induce a structural change in which base pairs or the loop of the T-Stem open. Further homonuclear Hartmann–Hahn spectroscopy experiments suggested that the loosely structured nature of the T-Stem is important for spermine binding.

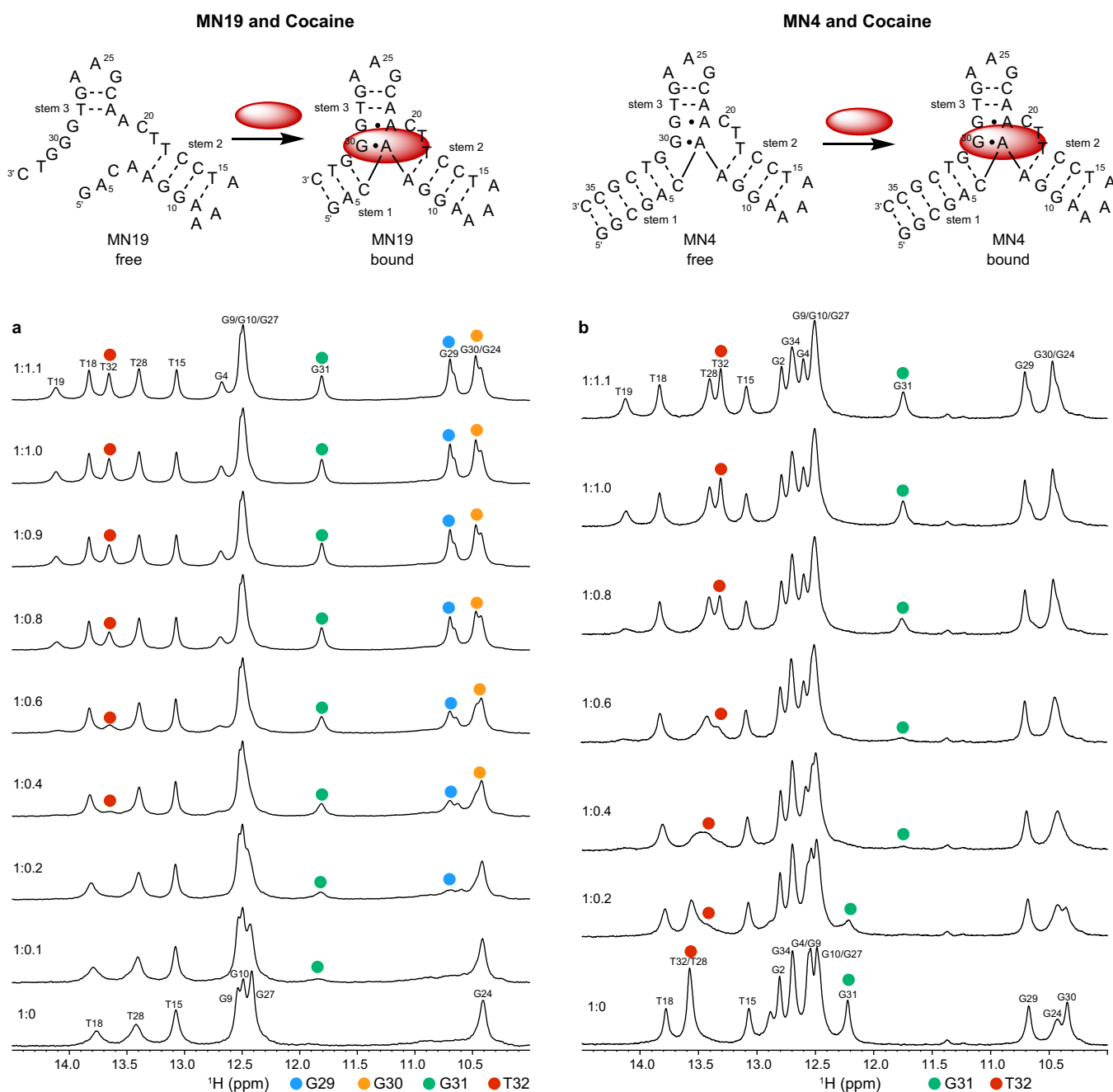


Figure 2. Cocaine binding by MN19 and MN4 cocaine-binding aptamers monitored by 1D ^1H NMR. The region of the NMR spectra shown focuses on the imino resonances. **(a)** Spectra of the MN19 cocaine-binding aptamer titrated with cocaine. **(b)** Spectra of the MN4 cocaine-binding aptamer titrated with cocaine. The NMR spectra of the MN19 aptamer demonstrates structural change with ligand binding by the appearance of new imino peaks for G29 (blue dot), G30 (orange dot), G31 (green dot), and T32 (red dot) that are not observed in the free spectrum. The NMR spectra of the prefolded MN4 aptamer shows chemical shift changes in imino peaks for G31 (green dot) and T32 (red dot) but not the appearance of new peaks. Spectra were acquired at 1.6 mM for MN19 and 1.0 mM for MN4 at 5°C in 5 mM KH_2PO_4 , 245 mM KCl (pH 6.8) and 90% $\text{H}_2\text{O}/10\%$ $^2\text{H}_2\text{O}$. The molar ratios of aptamer to cocaine are indicated.

1D ^1H NMR can also be employed to study G-quadruplex forming aptamers in the presence of their ligand. Bing *et al.* (2017) conducted a 1D ^1H NMR study to investigate the structural changes of the codeine-binding aptamer with its target. The ^1H NMR spectra of the free aptamer had broad and small peaks between 10 and 12 ppm. This indicated that the unbound aptamer may adopt several different quadruplex species. The spectrum also had broad peaks between 8.6–8.8 ppm and 13–14 ppm that were consistent with a triplex. With the addition of codeine, the NMR spectral peaks

narrowed and became well-resolved, showing a quadruplex and triplex. These NMR spectral changes suggested that codeine binding induces the aptamer to form a well-defined triplex-quadruplex structure. Similarly, Xu *et al.* (2022) performed 1D ^1H NMR to examine the structural changes of a 36-nucleotide ochratoxin-binding aptamer with its target. The ^1H NMR spectra of the free aptamer showed broad imino proton signals between 10 and 14 ppm, suggesting the existence of duplex and G-quadruplex forms without a defined structure. In the presence of ochratoxin, the imino proton

signals sharpened and new peaks became visible between 10 and 14 ppm. This suggested that ochratoxin binding induces the aptamer to adopt a well-defined, stabilized duplex-quadruplex structure.

Isothermal titration calorimetry

Isothermal titration calorimetry (ITC) is a powerful label-free method to quantify the affinity and thermodynamic parameters of target binding by aptamers (Feig, 2007; Slavkovic and Johnson, 2018, 2023). ITC measures the heat change that occurs during an aptamer–ligand binding interaction by titration of ligand into a sample cell containing the aptamer. The resulting ITC thermogram gives the total heat change per injection and allows determination of the binding constant, stoichiometry, and enthalpy change. ITC can be used to demonstrate a ligand-induced folding mechanism of an aptamer–ligand pair by experimentally determining its isobaric heat capacity of binding (ΔC_p). ITC is performed to measure the enthalpy change of ligand binding (ΔH) by the aptamer over a range of temperatures (Velázquez-Campoy *et al.*, 2004). The enthalpy changes are plotted as a function of temperature and fit to a linear plot. The change in heat capacity ($\Delta C_p = \Delta H/\Delta T$) can be obtained from the slope of this line.

Burial of nonpolar surfaces away from an aqueous solvent is associated with a negative ΔC_p value (Spolar and Record Jr., 1994). During ligand binding, both burial of the ligand and ligand-induced folding of the aptamer can result in a reduction in the solvent accessible nonpolar surface area (Lin *et al.*, 2008). The magnitude of the ITC-derived ΔC_p of one aptamer can be compared with another aptamer when binding the same ligand. This comparison is especially relevant when considering two aptamers derived from the same parent aptamer, such as the MN4/MN19 cocaine-binding aptamer pair (Figure 2). The ligand would be expected to bury a similar apolar surface area when binding these related aptamers. Therefore, the aptamer with a greater negative ΔC_p may undergo ligand-induced folding and conformational rearrangements that

bury more of its nonpolar surface. This method has been applied to studying the cocaine, adenosine and runt domain-binding aptamers among others (Neves *et al.*, 2010; Reinstein *et al.*, 2011, 2013; Amano *et al.*, 2016; Zhang *et al.*, 2017).

Reinstein *et al.* (2013) investigated quinine binding by the MN19 and MN4 cocaine-binding aptamers through determining their changes in heat capacity from ITC experiments. The MN19 aptamer, with a three base-pair stem 1, was found to have a more negative ΔC_p when binding quinine than the MN4 aptamer with a six base-pair stem 1 (Table 1). Quinine is thought to have comparable apolar surface area burial when binding both aptamers. Thus, the larger magnitude of ΔC_p for MN19 was attributed to a ligand-induced folding mechanism that involves more nonpolar surface area of the aptamer being buried with aptamer folding, upon quinine binding. In contrast, the MN4 aptamer is prefolded prior to quinine binding. A similar trend was observed with a larger negative ΔC_p obtained for the short stem 1 MN6 cocaine-binding aptamer binding cocaine and the short stem 1 MS2 aptamer binding deoxycholic acid (Table 1) (Neves *et al.*, 2010; Reinstein *et al.*, 2011). For each of these cocaine-binding aptamers with a short stem 1, the more negative ΔC_p provides evidence of aptamer folding with ligand binding.

Zhang *et al.* (2017) studied the binding mechanism of a two-site adenosine triphosphate (ATP)-binding DNA aptamer named Apt2a and a single-site variant aptamer named Apt1a. The enthalpy changes of Apt2a and Apt1a binding adenosine were measured over a range of temperatures by ITC to obtain their heat capacity changes. Apt2a had a greater magnitude of negative ΔC_p than Apt1a (Table 1), indicating a relatively larger conformational rearrangement of Apt2a with adenosine binding than Apt1a. Similarly, Amano *et al.* (2016) examined binding of the AML1 transcription factor runt domain (RD) to the aptamers named S4-S and RDE. Both aptamers exhibited ligand-induced conformational changes with a large negative ΔC_p . The greater magnitude of ΔC_p for the S4-S aptamer relative to the RDE aptamer indicates that more apolar surface area burial and structural change took place upon S4-S binding RD.

Table 1. ITC-derived heat capacity changes (ΔC_p) of aptamer–ligand binding interactions

Aptamer	Ligand	ΔC_p (cal mol ⁻¹ K ⁻¹)	Binding notes	Reference
MN4	Cocaine	-557 ± 29	Prefolded	Neves <i>et al.</i> , 2010
MN6	Cocaine	-922 ± 51	Ligand-induced folding	Neves <i>et al.</i> , 2010
MN4	Quinine	-377 ± 55	Prefolded	Reinstein <i>et al.</i> , 2013
MN19	Quinine	-798 ± 91	Ligand-induced folding	Reinstein <i>et al.</i> , 2013
WC	Deoxycholic acid	-94 ± 75	Prefolded	Reinstein <i>et al.</i> , 2011
MS2	Deoxycholic acid	-753 ± 200	Ligand-induced folding	Reinstein <i>et al.</i> , 2011
Apt1a	Adenosine	-340	1 binding site stabilized	Zhang <i>et al.</i> , 2017
Apt2a	Adenosine	-720	2 binding sites stabilized, internal bubble/bulge	Zhang <i>et al.</i> , 2017
RDE	AML1 transcription factor runt domain	-520 ± 50	Smaller conformational change of aptamer	Amano <i>et al.</i> , 2016
S4-S	AML1 transcription factor runt domain	-820 ± 140	Greater conformational change of aptamer	Amano <i>et al.</i> , 2016
Malachite green aptamer	Malachite green	-1,130	Greater conformational change of aptamer	Sokoloski <i>et al.</i> , 2012
Malachite green aptamer	Tetramethylrosamine	-450	Smaller conformational change of aptamer	Sokoloski <i>et al.</i> , 2012
Purine riboswitch	Purine	-810	Binding site rearrangement	Gilbert <i>et al.</i> , 2006
Tyrosinamide aptamer	Tyrosinamide	-495	Conformational change, induced fit	Lin <i>et al.</i> , 2008
L-argininamide aptamer	L-argininamide	-116 ± 29	Binding site stabilization, 2 bp stabilized	Bishop <i>et al.</i> , 2007

Another way to investigate ligand-induced conformational changes is to compare ITC-derived ΔC_p values for two different ligands binding the same aptamer. Sokoloski *et al.* (2012) performed ITC to obtain heat capacity changes for malachite green (MG) and tetramethylrosamine (TMR) binding to the malachite green RNA aptamer. The binding of MG was found to have a 2.5-fold larger magnitude for its negative heat capacity change than TMR (Table 1). This indicates that greater conformational changes occurred with the aptamer binding MG compared to TMR. This result was consistent with their finding that the MG-bound aptamer had a greater change in solvent accessible surface area than the TMR-bound aptamer by 250 Å². This change in surface area represented 4.8% of the total accessible surface area.

The ITC-derived ΔC_p values of various aptamer–ligand binding pairs are summarized in Table 1 along with whether structural change occurs during their binding interactions. There is no specific threshold or cut-off value for negative ΔC_p that indicates whether an aptamer is structure-switching or not. Thus, it is best to compare the relative magnitude of negative ΔC_p for pairs of aptamers binding the same ligand rather than evaluating the absolute ΔC_p values of aptamers. When comparing two aptamers binding the same ligand, the aptamer with a significantly larger negative ΔC_p indicates that it undergoes greater conformational change with ligand binding. This trend is observed between pairs of MN4 and MN19 aptamers binding quinine, the WC and MS2 aptamers binding deoxycholic acid and the Apt1a and Apt2a aptamers binding adenosine (Table 1).

Circular dichroism spectroscopy

Circular dichroism (CD) spectroscopy is a low-resolution structural technique that is used to study the secondary structure of macromolecules (Chang *et al.*, 2012). CD spectroscopy measures the difference in the absorption of right-handed and left-handed circularly polarized light by optically active biological molecules, such as proteins and nucleic acids. Distinct CD spectral patterns have been identified for various nucleic acid secondary structures, including A-form, B-form, and Z-form helices as well as for the different arrangements formed by DNA G-quadruplexes. These characteristic spectra have peaks in molar ellipticity at particular wavelengths (Kypr *et al.*, 2009; Chang *et al.*, 2012). For example, parallel G-quadruplexes typically have CD spectra with a maximum at 260 nm (Kypr *et al.*, 2009; Chang *et al.*, 2012). In contrast, antiparallel G-quadruplexes have CD spectra with a maximum at 295 nm and a minimum at 260 nm. Structure-switching DNA aptamers may undergo conformational changes between different secondary structures as a result of ligand binding. Therefore, CD spectroscopy can be used to effectively monitor these ligand-induced structural changes by comparing the CD spectra of free and ligand-bound aptamers.

One way that CD spectroscopy can indicate ligand-induced conformational changes of an aptamer is by a shift in the wavelength of peaks between the free and ligand-bound CD spectra (Lin *et al.*, 2011; Nakatsuka *et al.*, 2018). Lin *et al.* (2011) used CD to study the secondary structural changes of a 15-nucleotide thrombin-binding aptamer upon binding thrombin. CD spectra of the aptamer alone showed a minimum at 245 nm and a maximum at 280 nm, indicating a B-form DNA conformation. When thrombin was added, shifts of these minimum and maximum peaks occurred to 260 nm and 295 nm, respectively. A new maximum in the CD spectra also became visible at 254 nm. This suggested that the aptamer undergoes a conformational change from B-form DNA to an antiparallel G-quadruplex when binding thrombin (Kypr

et al., 2009; Lin *et al.*, 2011). Similarly, Nakatsuka *et al.* (2018) used CD to investigate the secondary structural rearrangements of a dopamine-binding aptamer upon binding its target. CD spectral shifts showed that dopamine binding by the aptamer causes it to change from a duplex to a different secondary structure. A shift in wavelength indicating structural change with ligand binding by an aptamer was also seen for the vancomycin-binding aptamer vanc-4-trunc (Dauphin-Ducharme *et al.*, 2019).

In addition to CD spectral shifts, changes in the intensity of CD peaks at a given wavelength can indicate conformational changes of aptamers (Chang *et al.*, 2012; Mehennaoui *et al.*, 2019; Aljohani *et al.*, 2020; Xie *et al.*, 2022; Xu *et al.*, 2022; Wu *et al.*, 2023; Alkhamis *et al.*, 2024). Xie *et al.* (2022) used CD to demonstrate the target-induced structural changes of several truncated methamphetamine (MAMP)-binding aptamers. The researchers removed bases from both ends of the original MAMP-binding aptamer to generate destabilized 36 and 38 oligonucleotide versions. CD was performed on the aptamer variants in the free and target-bound states to characterize their conformational changes. Both truncated variants showed an increase in the intensity of a CD maximum at 290 nm with MAMP addition, suggesting structural changes with MAMP binding. The 38-oligonucleotide variant had the largest peak intensity increase, indicating that it undergoes the greatest conformational change of the variants studied. Furthermore, Xu *et al.* (2022) conducted CD experiments to monitor the structural changes of a 33-oligonucleotide ochratoxin A (OTA)-binding aptamer. CD spectra of the free OTA-binding aptamer showed the general pattern of an antiparallel G-quadruplex in the presence of Na⁺ and Mg²⁺ ions. A significant increase in the intensity of a CD minimum around 260 nm was observed upon OTA addition. This provided evidence in combination with NMR studies that OTA binding induces the aptamer to form a well-defined unique antiparallel G-quadruplex structure. Similarly, Yang *et al.* (2011) and Fadock and Manderville (2017) performed CD experiments that demonstrate antiparallel G-quadruplex formation of the OTA-binding aptamer with OTA addition. Finally, an example of an aptamer going from unstructured in the free state, with no discernable peaks in the CD spectrum, to a structured ligand-bound aptamer is the methotrexate-binding aptamer from the Plaxco group (Wu *et al.*, 2023).

Thermal melt analysis

Ultraviolet–visible (UV) absorption spectroscopy is a classic biophysical method that can be used to study the thermal stability of macromolecules by monitoring their unfolding when heated (Mergny and Lacroix, 2003). Duplex nucleic acids have a maximum UV absorption at 260 nm and exhibit hyperchromicity as their absorbance at 260 nm increases upon denaturation. During a thermal unfolding experiment monitored by UV, the absorbance of a nucleic acid sample at 260 nm is measured as a function of temperature as shown in Figure 3. A sigmoidal thermal melt curve indicates the transition of the nucleic acid from a folded duplex conformation to an unfolded single-stranded state (solid line; Figure 3). However, a straight line thermal melt suggests that the nucleic acid originally exists in a single-stranded state and little or no unfolding occurs during heating (dashed line; Figure 3). UV melting curves can be obtained individually for free and ligand-bound aptamers and compared. A change from a straight line UV melt curve for a free aptamer to a sigmoidal UV melt curve for a ligand-bound aptamer provides evidence of ligand-induced folding of the aptamer.

Neves *et al.* (2017) used UV-spectroscopy to investigate how the length of stem 1 of the three-way junction cocaine-binding aptamer

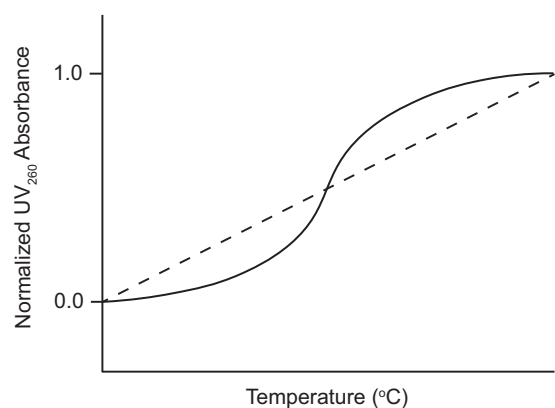


Figure 3. Example of UV thermal melt curves of an aptamer that undergoes ligand-induced folding. UV thermal melt curve of an unfolded free aptamer shown by the dashed line. UV thermal melt curve of a folded ligand-bound aptamer shown by the solid line.

affects its ligand-induced conformational change. The authors performed UV thermal melts on cocaine-binding aptamers with different lengths of stem 1. For the OR8 aptamer with a stem 1 of two base pairs and the MN19 aptamer with a stem 1 of three base pairs, the free aptamers exhibited straight line UV thermal melts rather than sigmoidal curves. This suggested that OR8 and MN19 aptamers are not completely folded in their unbound state, but rather loosely or partially folded. Hence, there is no visible transition to an unfolded state when the temperature increases. In contrast, UV melts of these two aptamers bound to quinine exhibited sigmoidal denaturation curves with measurable melt temperatures (Neves *et al.*, 2017). This indicated that OR8 and MN19 aptamers are folded when bound to the ligand quinine and transition to an unfolded state during heating. Overall, these results provide support for the ligand-induced folding mechanism of OR8 and MN19 cocaine-binding aptamers and provide a guide when looking at other aptamers that may undergo ligand-induced folding.

Differential scanning calorimetry (DSC) is a technique that can be used in a complementary fashion to UV-based melts to measure the thermal stability of both free and ligand-bound aptamers. In addition to an unfolding temperature, DSC also provides a wealth of thermodynamic data for folding and unfolding. DSC methods have been applied to the cocaine-binding aptamer system of MN4 and MN19 to investigate the difference between an unfolded unbound aptamer (free MN19) and a folded bound aptamer (cocaine or quinine-bound MN19). There was a negligible unfolding signal for the free MN19 aptamer while an unfolding peak was observed, as expected, for the structured ligand-bound MN19 aptamer (Harkness *et al.*, 2016).

Small-angle X-ray scattering

Small-angle X-ray scattering (SAXS) is a method used to characterize the global structure of biological macromolecules by providing information on their molecular size, shape, and oligomeric state (Baird and Ferré-D'Amaré, 2014). In a SAXS experiment, the intensities of scattered X-rays by a sample of the biological molecule are measured as a function of the scattering angle. From the SAXS data, parameters such as the radius of gyration (R_g) can be obtained as an indication of the overall size of the biological molecule (Kikhney and Svergun, 2015). The R_g represents the root mean square distance of the molecule in relation to its centre of mass. SAXS data can also be used to produce a pairwise distance

distribution function (PDDF), which represents the distribution of distances between pairs of atoms within the macromolecule and provides its maximum diameter (D_{max}). Additionally, SAXS data can be utilized to generate three-dimensional *ab initio* low-resolution reconstructions of the shape of the biomolecule. SAXS can effectively provide insight into ligand-induced folding and compaction of aptamers by comparing SAXS-derived R_g , PDDFs and *ab initio* models of free and ligand-bound aptamers.

SAXS has been widely used to investigate the conformational changes of riboswitches in response to metabolite binding (Lipfert *et al.*, 2007; Baird and Ferré-D'Amaré, 2010; Baird *et al.*, 2010; Chen *et al.*, 2011). Chen *et al.* (2011) used SAXS to follow the structural changes of the SAM-II riboswitch in response to binding its metabolite S-adenosyl methionine (SAM). Upon addition of SAM, the riboswitch undergoes compaction with a decreased R_g from 31.7 to 20.7 Å and reduced D_{max} from 112 Å to 70 Å. Low resolution *ab initio* modeling revealed that the aptamer domain of the unbound riboswitch exists in an elongated conformation whereas the aptamer domain of the riboswitch bound to SAM exhibits a more compact structure. Complementary 1D NMR experiments demonstrated that the SAM-II riboswitch compaction induced by metabolite-binding is associated with secondary and tertiary structural changes.

Baird and Ferré-D'Amaré (2010) also performed SAXS to study the global structural changes of the *E. coli thiM* thiamine pyrophosphate (TPP)-responsive riboswitch aptamer domain with metabolite binding. At physiologic Mg^{2+} concentrations, the TPP-responsive riboswitch alone had an R_g of 27.5 Å and addition of its metabolite TPP resulted in a reduced R_g of 24.1 Å. Low-resolution *ab initio* reconstructions from SAXS data supported this ligand-induced compaction as it showed that the unbound TPP-responsive riboswitch had a more elongated form than the riboswitch bound to its metabolite. Thus, SAXS experiments suggested that the *thiM* TPP-responsive riboswitch aptamer domain acquires distinct free and metabolite-bound conformations. Baird and Ferré-D'Amaré (2010) and Baird *et al.* (2010) also used SAXS to show that the class I SAM-responsive riboswitch and cyclic diguanylate riboswitch aptamer domains undergo compaction and global conformational changes upon binding their metabolites.

In addition to its application in studying riboswitches, SAXS has been used to investigate the conformational changes of *in vitro* selected DNA aptamers in response to ligand binding. Reinstein *et al.* (2013) performed SAXS to study the ligand-induced folding of the MN19 cocaine-binding aptamer in comparison to the prefolded MN4 cocaine-binding aptamer. PDDFs for the MN19 aptamer showed notable differences between its free, quinine-bound and cocaine-bound forms. For example, a shoulder at approximately 35 Å was visible in the PDDF of the free MN19 aptamer but absent in the quinine-bound and cocaine-bound forms of the aptamer. Additionally, a larger amount of variation was found among SAXS-derived *ab initio* reconstructions for these three forms of the MN19 aptamer compared to the MN4 aptamer. Together, these SAXS findings provide support for the ligand-induced conformational changes of the MN19 aptamer when binding quinine and cocaine.

Schmidt *et al.* (2020) also used SAXS to investigate the interaction of the L-RNA aptamer NOX-B11 with its target, active ghrelin. SAXS-derived *ab initio* reconstructions of the NOX-B11 aptamer alone showed an elongated structure with a length of about 7.7 nm and diameter of 4 nm. In contrast, *ab initio* models of the NOX-B11-ghrelin complex revealed a more compact structure with a shorter length of about 5.8 nm and diameter of 4.2 nm. PDDFs

also demonstrated that the NOX-B11-ghrelin complex is more compact as it had a smaller D_{\max} of approximately 6.2 nm relative to NOX-B11 alone with a D_{\max} of 7.8 nm. Overall, these SAXS data reveal that the NOX-B11 aptamer undergoes a conformational change to a more compact form as a result of binding ghrelin.

Native ion mobility-mass spectrometry

Native mass spectrometry coupled to ion mobility (IM-MS) is a valuable biophysical method to study non-covalent assemblies in the gas-phase, including aptamer–ligand interactions (Konijnenberg *et al.*, 2013; Largy *et al.*, 2022). Electrospray ionization can take biomolecular complexes from solution into the gas-phase with their native conformation retained for passage through ion mobility and mass spectrometers. Native IM-MS provides insight into the binding stoichiometry as well as the size, shape, and mass of the non-covalent complex (Allison *et al.*, 2020).

Daems *et al.* (2021) used native IM-MS to study quinine-binding by a set of different cocaine-binding aptamers. Native IM-MS measurements were taken for free and quinine-bound aptamers in 5+ ionization modes and their arrival times were extracted as a measure of ion mobility. Significant arrival time increases were observed for the aptamer–quinine complexes relative to free aptamers. The addition of quinine to the total volume of the aptamer–quinine complex could not alone account for these arrival time differences. Daems *et al.* proposed that the increased arrival times were partly due to conformational changes of the aptamer with ligand binding that causes a slight elongation of its gas-phase structure. Specifically, the MN19 aptamer had an arrival time increase of 6.4% whereas the MN4 aptamer had a smaller arrival time increase of 4.2%. The larger arrival time difference for the MN19 aptamer suggested that its loosely folded-free structure undergoes greater structural change when binding quinine. In contrast, the MN4 aptamer with a more rigid, prefolded structure undergoes less conformational change with ligand binding as shown by its smaller arrival time difference. These results are consistent with NMR, ITC, and SAXS studies discussed earlier in this review that demonstrate the ligand-induced conformational changes of the MN19 aptamer (Neves *et al.*, 2010; Reinstein *et al.*, 2013).

Fluorescence-based methods

Aptamers are frequently employed in fluorescent biosensors to detect and quantify specific ligand concentrations (Wang *et al.*, 2011). These fluorescence-based methods are more often used as a detection method for an analyte rather than a method to demonstrate the occurrence of structural change with ligand binding. In these applications, the aptamer is often tagged, and structural change is assumed to occur based on the change in fluorescent output. These sensors can produce a measurable change in fluorescence that coincides with a fluorescently labeled aptamer's conformational changes upon target binding. In this way, the fluorescence output indicates the extent of ligand binding and allows measurement of ligand concentrations. Fluorescent biosensors often use fluorescence quenching or de-quenching and fluorescence resonance energy transfer (FRET) as distance-dependent phenomena to report on an aptamer's structural changes with ligand binding.

Fluorescence quenching occurs when an excited fluorophore in close proximity to a non-fluorescent quencher transfers its energy to the quencher without emission of light (Lyklema, 2000). This

phenomenon is measured as a decrease in fluorescence intensity of the fluorophore's emission by fluorescence spectroscopy. Alternatively, when a fluorophore is moved away from a quencher, fluorescence de-quenching takes place, and the fluorescence intensity of the fluorophore increases. FRET, on the other hand, involves a transfer of energy from an excited donor fluorophore to a second nearby acceptor fluorophore that then emits fluorescence (Kaur *et al.*, 2020; Lyklema, 2000). For FRET to happen, the emission spectrum of the donor must have sufficient overlap with the absorption spectrum of the acceptor and the two fluorophores must be about 1–10 nm apart. FRET is detected by a reduction in the excited donor's fluorescence intensity and an increase in the acceptor's emission fluorescence intensity by fluorescence spectroscopy. The ratio of fluorescence emission between the two fluorophores serves as a measure of the FRET signal. Fluorescence quenching and FRET can both be used to monitor structural changes of aptamers upon ligand binding in fluorescent sensors. Feagin *et al.* (2018) classified the use of structure-switching aptamers in fluorescent biosensors into several types of applications, including aptamer beacons, strand-displacement methods, and split aptamers (Feagin *et al.*, 2018). It is possible that measurement of fluorescent lifetime, as opposed to intensity, may be used as a way to probe changes in fluorescent properties.

Fluorescence quenching and FRET-based aptamer beacon sensors

Many structure-switching aptamers have been employed in fluorescent aptamer beacons. In an aptamer beacon, ligand binding to an aptamer causes conformational changes that alter the distance between the aptamer's covalently attached fluorophore and quencher or second fluorophore, resulting in a measurable change in fluorescence (Figure 4) (Perez-Gonzalez *et al.*, 2016). Hamaguchi *et al.* (2001) used the thrombin-binding aptamer to design a fluorescent turn-on aptamer beacon that detects thrombin (Figure 4).

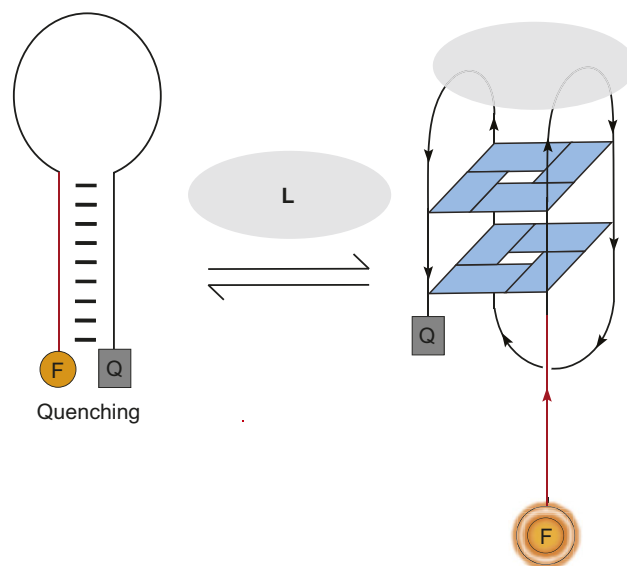


Figure 4. Fluorescent turn-on aptamer beacon. Structural change of aptamer with ligand binding results in an increase in fluorescent output (i.e., fluorescence de-quenching) by separating its fluorophore and quencher-labeled ends (complementary nucleotides added to the 5' end of the thrombin-binding aptamer are shown in red) (Hamaguchi *et al.*, 2001).

Complementary nucleotides were introduced to the 5' end of the aptamer to hybridize with its 3' end and form a closed hairpin. The fluorophore (fluorescein) and quencher (dabcyl) were attached to the 5' and 3' ends of the aptamer, respectively. It was hypothesized that the closed stem-loop would be stable in the absence of thrombin and thrombin-binding would shift the equilibrium toward a G-quadruplex structure in which the fluorophore and quencher become separated (Figure 4). Without thrombin, minimal fluorescence was detected due to fluorescence quenching in the closed hairpin. However, addition of thrombin to saturating concentrations resulted in a 2.5-fold enhancement in fluorescence intensity for the beacon construct that was extended by five nucleotides. This rise in fluorescence provided evidence of the thrombin-induced structural change of the aptamer from a closed hairpin to G-quadruplex conformation.

Li *et al.* (2002) also employed the thrombin-binding aptamer to construct their quenching-based turn-off aptamer beacon (Figure 5). Binding thrombin shifts the equilibrium of the aptamer from a random coil conformation to a G-quadruplex state. The two ends of the aptamer were labeled with carboxyfluorescein (FAM) as fluorophore and dabcyl as quencher such that they were far away in the random coil, but close together in the G-quadruplex conformation. Addition of thrombin was found to reduce the fluorescence intensity of the aptamer beacon by 60%. This indicated that the fluorophore and quencher came together by the thrombin-induced conformational change of the aptamer to a G-quadruplex. A similarly designed turn-off aptamer beacon that uses fluorescence quenching demonstrates the structure-switching binding mechanism of the dopamine-binding aptamer (Liu *et al.*, 2021).

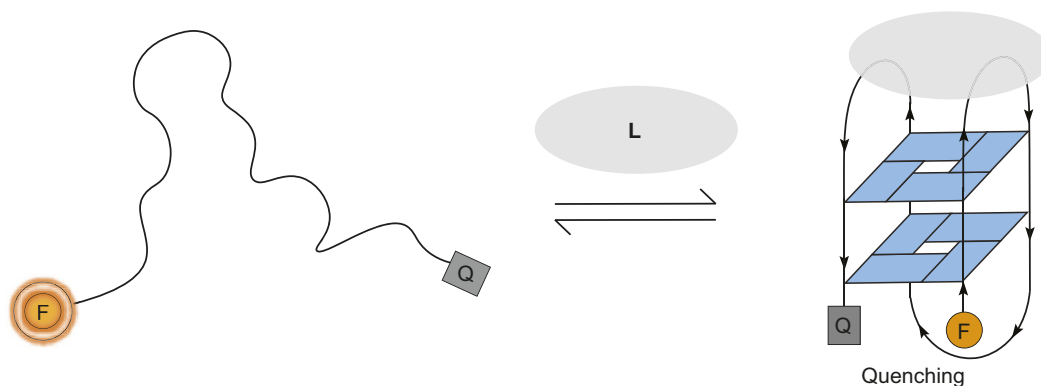


Figure 5. Fluorescent turn-off aptamer beacon. Conformational change of aptamer with ligand binding results in a decrease in fluorescent output (i.e., fluorescence quenching) by bringing together its fluorophore and quencher-labeled ends (Li *et al.*, 2002).

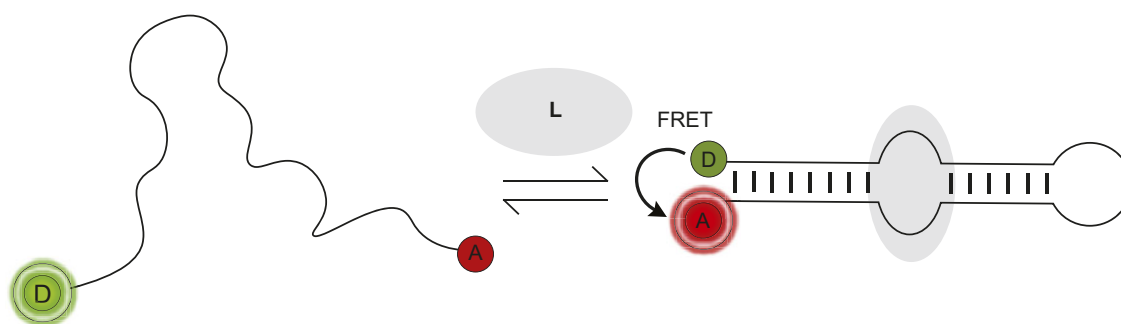


Figure 6. FRET-based aptamer beacon. Structural change of aptamer with ligand binding produces an increase in FRET signal by bringing together its donor and acceptor-labeled ends (Li *et al.*, 2008).

In addition, FRET-based aptamer beacons have been used to show ligand-induced conformational changes of a variety of aptamers (Li *et al.*, 2002, 2008; Ueyama *et al.*, 2002; Liu *et al.*, 2021). Li *et al.* (2008) designed a FRET-based biosensor using the angiogenin-binding aptamer (Figure 6). Binding angiogenin shifts the equilibrium of the aptamer from an unfolded random coil to a folded structure that resembles a stem-loop. In the aptamer beacon, the 5' and 3' ends of the aptamer were modified with FAM as the donor and carboxytetramethylrhodamine (TAMRA) as the acceptor, respectively. The labeled 5' and 3' termini were far apart in the random coil, but close together in the stem-loop secondary structure. When angiogenin was added, there was an enhanced FRET signal detected. The fluorescence intensity of the acceptor TAMRA at 577 nm increased while that of the donor FAM at 520 nm decreased in the presence of angiogenin. This provided evidence that angiogenin binding induced a structural change in the aptamer to a stem-loop that brought together its FAM and TAMRA-labeled termini for energy transfer. FRET-based aptamer beacons have also been designed using thrombin, dopamine and K^+ -binding aptamers and demonstrate their ligand-induced conformational changes (Li *et al.*, 2002; Ueyama *et al.*, 2002; Liu *et al.*, 2021).

Fluorescent aptamer sensors using complementary displacement strand

Nutiu *et al.* developed a general method for creating fluorescent signaling aptamers in which a DNA/DNA duplex changes structure to a DNA/ligand complex upon ligand binding (Figure 7) (Nutiu and

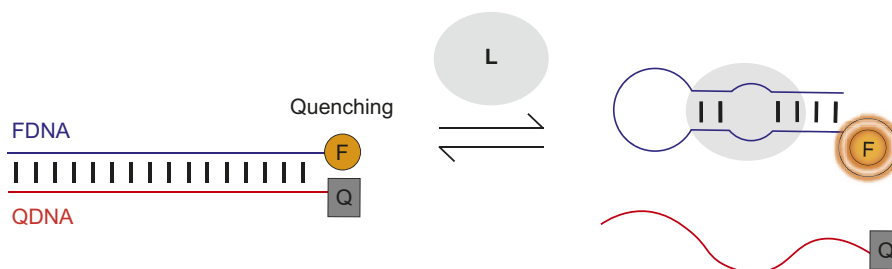


Figure 7. Fluorescent signaling aptamer using strand displacement. Ligand binding to aptamer labeled with fluorophore (FDNA) disrupts hybridization to a complementary strand labeled with quencher (QDNA) and results in an increase in fluorescence. A scheme similar to the one illustrated has been used with the ATP binding DNA aptamer (Nutiu and Li, 2003).

Li, 2003; Lau and Li, 2014). Their strategy makes use of a DNA aptamer labeled with fluorophore (FDNA) and a short oligonucleotide complementary to the aptamer labeled with quencher (QDNA). Without ligand, the aptamer hybridizes with QDNA to form a DNA/DNA duplex. In this conformation, the fluorophore and quencher are located near each other, resulting in fluorescence quenching. However, in the presence of ligand, QDNA is displaced from the aptamer by ligand binding and the aptamer–ligand complex forms. This ligand-induced structural change is shown by an increase in fluorescence intensity of the fluorophore upon ligand addition.

Qiao *et al.* (2021) applied this strand displacement strategy when designing a structure-switching sensor to detect the mycotoxin aflatoxin M1 (AFM1) in milk. The AFM1-binding aptamer was labeled with the fluorophore FAM and a complementary DNA (cDNA) was modified with the quencher TAMRA. Without AFM1, the FAM-labeled aptamer and TAMRA-labeled cDNA hybridize together, resulting in fluorescence quenching (Figure 7). However, when AFM1 was added, there was an 11-fold rise in fluorescence intensity. This fluorescence de-quenching upon AFM1 addition provided evidence of the ligand-induced structural change of TAMRA-cDNA dissociation and formation of the AFM1/aptamer complex. Structure-switching sensors involving displacement of a complementary oligonucleotide from an aptamer by ligand to generate a fluorescent or FRET signal have been used to detect the antibiotic kanamycin and cytokine interferon-gamma (Tuleuova *et al.*, 2010; Ma *et al.*, 2019). Nutiu and Li (2003) also successfully applied their complementary

displacement strand strategy to ATP and thrombin-binding aptamers using a tripartite system.

Split aptamer fluorescent and FRET-based sensors

Aptamers can be divided into two or more fragments (split) that associate upon ligand binding. The structural change of two aptamer strands coming together can be signified by changes in fluorescence or FRET signal using fluorescent-labeling of the strands. Stojanovic *et al.* (2000) designed a fluorescent sensor to detect cocaine based on the self-assembly of a split cocaine-binding aptamer (Figure 8). The three-way junction aptamer was divided into two fragments at a loop. The 5' end of one aptamer fragment was modified with the fluorophore FAM while the 3' end of the other aptamer fragment was labeled with the quencher dabcyl. It was predicted that the aptamer would exist primarily as two individual strands in the absence of cocaine and that cocaine addition would shift the equilibrium toward an assembled aptamer in which the fluorophore and quencher on the two strands come together. Upon cocaine addition, fluorescent emission by the fluorophore was quenched to 65% of its original emission without cocaine. This fluorescence quenching demonstrated the cocaine-induced assembly of individual aptamer subunits to form the complete aptamer. A split-aptamer system was also successfully used in a fluorescence quenching sensor to detect 19-nortestosterone (Bai *et al.*, 2016).

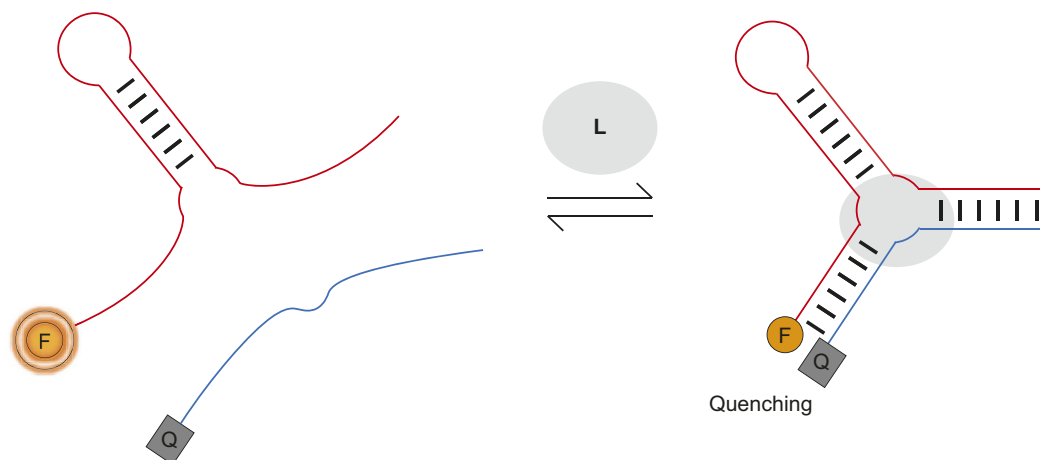


Figure 8. Split aptamer fluorescent sensor. Assembly of split aptamer fragments upon ligand binding results in a decrease in fluorescent output by bringing together their fluorophore and quencher-labeled ends. This scheme is adapted from one used for the cocaine-binding aptamer (Stojanovic *et al.*, 2000).

In addition, a FRET-based sensor was developed by Liu *et al.* (2014) using a split version of the thrombin-binding aptamer. The aptamer was divided into two strands, one of which was covalently modified with FAM as the FRET acceptor. A water-soluble polycationic polymer (PFEP) that has high emission of fluorescence served as the FRET donor. Without thrombin, the positively charged PFEP formed complexes with fragments of the split thrombin-binding aptamer through electrostatic interactions. An efficient FRET signal occurred between the closely interacting PFEP and FAM-labeled aptamer strand. When thrombin was added, the two split aptamer strands assembled into a G-quadruplex induced by thrombin binding. The large size of the bound thrombin increased the distance between the PFEP and FAM-labeled aptamer strand as part of the G-quadruplex, leading to a weakened FRET signal. This decrease in FRET signal served as evidence of the thrombin-induced conformational change of the split aptamer strands assembling into a G-quadruplex.

Conclusions

Here, we have reviewed different biophysical tools readily available to monitor changes in the structure of aptamers when they bind their ligand. These tools provide distinct information (Table 2) on these molecules which can prove essential information into their

designs and thus their translation in different applications, especially biosensors.

The related field of riboswitches can provide insight into future directions for the field of biophysical analysis of structure-switching aptamers (Kavita and Breaker, 2023). For riboswitches, many X-ray crystallography-based structures of free and bound molecules have been determined allowing for a detailed structural comparison between the free and bound structures. In contrast, there are relatively few structures of small molecule-binding aptamers, though this is not the case for protein-binding aptamers (Gelinas *et al.*, 2016). More high-resolution structural information on aptamers, especially on DNA aptamer-small molecule interactions, is necessary to provide further insights into aptamer–ligand interactions. However, if the goal is to provide evidence of large-scale structure switching, then this is not strictly necessary. Additionally, single molecule methods have been commonly applied to riboswitches (Boudreault *et al.*, 2015). While this type of analysis has been reported for aptamers (Morris *et al.*, 2018), it has not been widely applied for studying SELEX-derived aptamers (Morris *et al.*, 2018). Some classic biochemical methods such as chemical probing, for example, SHAPE analysis (Weeks, 2021), and electrophoresis-based techniques have not been widely employed and may provide complementary information with results provided by the techniques discussed in this review.

Table 2. Summary of biophysical methods to demonstrate structure-switching binding mechanism of aptamers

Structural and binding methods	Evidence of structure switching with ligand binding. Limitations and advantages of the method
1D ^1H NMR spectroscopy	Increase in number of and narrowing of imino proton signals between free and ligand-bound aptamer spectra. <i>Advantages:</i> nucleotide-specific structural information provided. <i>Limitations:</i> high level of expertise needed; relatively large amounts of material needed.
ITC	Large negative heat capacity change of ligand binding. <i>Advantages:</i> easy to perform experiments. <i>Limitations:</i> indirect method; relatively large amount of material needed.
CD spectroscopy	Change in wavelengths of maxima and minima or intensity of molar ellipticity between free and ligand-bound aptamer spectra. <i>Advantages:</i> quick and easy to perform experiments. <i>Limitations:</i> global, not local structural information provided.
UV-visible spectroscopy	Straight line thermal melt with no measurable melt temperature for unfolded free aptamer; Sigmoidal thermal melt with measurable melt temperature for folded ligand-bound aptamer. <i>Advantages:</i> quick and easy to perform experiments. <i>Limitations:</i> global, not local structural information provided.
SAXS	Change in radius of gyration, pair distance distribution function and/or <i>ab initio</i> reconstructions of aptamer between its free and ligand-bound forms. <i>Advantages:</i> small amount of material needed. <i>Limitations:</i> expensive and specialized equipment needed; high level of expertise needed; low resolution structural information.
Native IM-MS	Increase in arrival time upon ligand binding of aptamer in the gas phase compared to free aptamer. <i>Advantages:</i> very small amount of material needed. <i>Limitations:</i> high level of expertise needed; function of aptamer in gas phase not necessarily guaranteed.
Fluorescence-based methods	Evidence of structure switching with ligand binding. Limitations and advantages of the method
Aptamer beacon and split aptamer ^a	Increase ('turn on') or decrease ('turn off') in fluorescent output when two ends of a single aptamer or strands of a split aptamer labeled with fluorophore and quencher change distance upon ligand binding. <i>Advantages:</i> small amount of material needed; easy to perform experiments. <i>Limitations:</i> attachment of labels to aptamer can alter their function; fluorophore and quencher can interact with each other
Complementary strand displacement ^a	Increase in fluorescent output when ligand binding displaces a complementary strand labeled with quencher from a fluorophore-labeled aptamer. <i>Advantages:</i> small amount of material needed; easy to perform experiments. <i>Limitations:</i> attachment of labels to aptamer can alter their function; fluorophore and quencher can interact with each other

^aChanges in fluorescence resonance energy transfer (FRET) signal can be measured using two fluorophores instead of fluorescence quenching/de-quenching to demonstrate the structure-switching binding mechanism.

Each of the methods presented comes with its advantages and limitations (Table 2). While a single method can provide evidence of structural change, we advise the use of two or more methods for the most robust demonstration of ligand-induced structure switching. We anticipate that having a deeper understanding of the different capabilities of these methods can help researchers in rapidly acquiring insights into aptamer structure switching and further accelerate aptamer-based biosensor developments.

Acknowledgements. We thank past and present members of the Johnson Lab for critical reading of the manuscript.

Financial support. This work was supported by NSERC Discovery grants to P.D.D. and P.E.J.

Competing interest. The authors declare none.

References

- Aljohani MM, Chinnappan R, Alsager OA, Alzabn R, Alhoshani A, Weber K, Cialla-May D, Popp J and Zourob M (2020) Mapping the binding region of aptamer targeting small molecule: Dabigatran etexilate, an anti-coagulant. *Talanta* **218**, 121132.
- Alkhamis O, Canoura J, Ly PT and Xiao Y (2023) Using exonucleases for aptamer characterization, engineering, and sensing. *Accounts of Chemical Research* **56**, 1731–1743.
- Alkhamis O, Canoura J, Wu Y, Emmons NA, Wang Y, Honeywell KM, Plaxco KW, Kippin TE and Xiao Y (2024) High-affinity aptamers for in vitro and in vivo cocaine sensing. *Journal of the American Chemical Society* **146**, 3230–3240.
- Allison TM, Barran P, Cianféranis S, Degiacomi MT, Gabelica V, Grandori R, Marklund EG, Menneteau T, Migas LG, Politis A, Sharon M, Sobott F, Thalassinou K and Benesch JLP (2020) Computational strategies and challenges for using native ion mobility mass spectrometry in biophysics and structural biology. *Analytical Chemistry* **92**, 10872–10880.
- Amano R, Takada K, Tanaka Y, Nakamura Y, Kawai G, Kozu T and Sakamoto T (2016) Kinetic and thermodynamic analyses of interaction between a high-affinity RNA aptamer and its target protein. *Biochemistry* **55**, 6221–6229.
- Bai W, Zhu C, Liu J, Yan M, Yang S and Chen A (2016) Split aptamer-based sandwich fluorescence resonance energy transfer assay for 19-nortestosterone. *Microchimica Acta* **183**, 2533–2538.
- Baird NJ and Ferré-D'Amaré AR (2010) Idiosyncratically tuned switching behavior of riboswitch aptamer domains revealed by comparative small-angle X-ray scattering analysis. *RNA* **16**, 598–609.
- Baird NJ and Ferré-D'Amaré AR (2014) Analysis of riboswitch structure and ligand binding using small-angle X-ray scattering (SAXS). In Lafontaine D and Dubé A (eds), *Therapeutic Applications of Ribozymes and Riboswitches: Methods and Protocols*. Totowa, NJ: Humana Press, pp. 211–225.
- Baird NJ, Kulshina N and Ferré-D'Amaré AR (2010) Riboswitch function: Flipping the switch or tuning the dimmer? *RNA Biology* **7**, 328–332.
- Bing T, Zheng W, Zhang X, Shen L, Liu X, Wang F, Cui J, Cao Z and Shangquan D (2017) Triplex-quadruplex structural scaffold: A new binding structure of aptamer. *Scientific Reports* **7**, 15467.
- Bishop GR, Ren J, Polander BC, Jeanfreau BD, Trent JO and Chaires JB (2007) Energetic basis of molecular recognition in a DNA aptamer. *Biophysical Chemistry* **126**, 165–175.
- Boudreaux J, Perez-Gonzalez DC, Penedo JC and Lafontaine DA (2015) Single-molecule approaches for the characterization of riboswitch folding mechanisms. *Methods in Molecular Biology* **1334**, 101–107.
- Canoura J, Wang Z, Yu H, Alkhamis O, Fu F and Xiao Y (2018) No structure-switching required: A generalizable exonuclease-mediated aptamer-based assay for small-molecule detection. *Journal of the American Chemical Society* **140**, 9961–9971.
- Cánovas R, Daems E, Campos R, Schellinck S, Madder A, Martins JC, Sobott F and De Wael K (2022) Novel electrochemiluminescent assay for the aptamer-based detection of testosterone. *Talanta* **239**, 123121.
- Cekan P, Jonsson EO and Sigurdsson ST (2009) Folding of the cocaine aptamer studied by EPR and fluorescence spectroscopies using the bifunctional spectroscopic probe Ç. *Nucleic Acids Research* **37**, 3990–3995.
- Chang Y-M, Chen CK-M and Hou M-H (2012) Conformational changes in DNA upon ligand binding monitored by circular dichroism. *International Journal of Molecular Sciences* **13**, 3394–3413.
- Chen B, Zuo X, Wang Y-X and Dayie TK (2011) Multiple conformations of SAM-II riboswitch detected with SAXS and NMR spectroscopy. *Nucleic Acids Research* **40**, 3117–3130.
- Churcher ZR, Garaev D, Hunter HN and Johnson PE (2020) Reduction in dynamics of base pair opening upon ligand binding by the cocaine-binding aptamer. *Biophysical Journal* **119**, 1147–1156.
- Daems E, Dewaele D, Barylyuk K, De Wael K and Sobott F (2021) Aptamer–ligand recognition studied by native ion mobility-mass spectrometry. *Talanta* **224**, 121917.
- Dauphin-Ducharme P, Yang K, Arroyo-Currás N, Ploense KL, Zhang Y, Gerson J, Kurnik M, Kippin TE, Stojanovic MN and Plaxco KW (2019) Electrochemical aptamer-based sensors for improved therapeutic drug monitoring and high-precision, feedback-controlled drug delivery. *ACS Sensors* **4**, 2832–2837.
- Dayie TK, Olenginski LT and Taiwo KM (2022) Isotope labels combined with solution NMR spectroscopy make visible the invisible conformations of small-to-large RNAs. *Chemical Reviews* **122**, 9357–9394.
- Debiasi M, Lelievre A, Smietana M and Müller S (2020) Splitting aptamers and nucleic acid enzymes for the development of advanced biosensors. *Nucleic Acids Research* **48**, 3400–3422.
- Derosa MC, Lin A, Mallikaratchy P, McConnell EM, Mckeague M, Patel R and Shigdar S (2023) In vitro selection of aptamers and their applications. *Nature Reviews Methods Primers* **3**, 54.
- Fadock KL and Manderville RA (2017) DNA aptamer–target binding motif revealed using a fluorescent guanine probe: Implications for food toxin detection. *ACS Omega* **2**, 4955–4963.
- Feagin TA, Maganzini N and Soh HT (2018) Strategies for creating structure-switching aptamers. *ACS Sensors* **3**, 1611–1615.
- Feig AL (2007) Applications of isothermal titration calorimetry in RNA biochemistry and biophysics. *Biopolymers* **87**, 293–301.
- Gelinis AD, Davies DR and Janjic N (2016) Embracing proteins: Structural themes in aptamer–protein complexes. *Current Opinion in Structural Biology* **36**, 122–132.
- Gilbert SD, Stoddard CD, Wise SJ and Batey RT (2006) Thermodynamic and kinetic characterization of ligand binding to the purine riboswitch aptamer domain. *Journal of Molecular Biology* **359**, 754–768.
- Hamaguchi N, Ellington A and Stanton M (2001) Aptamer beacons for the direct detection of proteins. *Analytical Biochemistry* **294**, 126–131.
- Harkness V, Slavkovic RW, Johnson S and Mittermaier AK (2016) Rapid characterization of folding and binding interactions with thermolabile ligands by DSC. *Chemical Communications* **52**, 13471–13474.
- Huang P-JJ and Liu J (2022) Selection of aptamers for sensing caffeine and discrimination of its three single demethylated analogues. *Analytical Chemistry* **94**, 3142–3149.
- Kaur A, Kaur P and Ahuja S (2020) Förster resonance energy transfer (FRET) and applications thereof. *Analytical Methods* **12**, 5532–5550.
- Kavita K and Breaker RR (2023) Discovering riboswitches: The past and the future. *Trends in Biochemical Sciences* **48**, 119–141.
- Kent AD, Spiropoulos NG and Heemstra JM (2013) General approach for engineering small-molecule-binding DNA split aptamers. *Analytical Chemistry* **85**, 9916–9923.
- Kikhney AG and Svergun DI (2015) A practical guide to small angle X-ray scattering (SAXS) of flexible and intrinsically disordered proteins. *FEBS Letters* **589**, 2570–2577.
- Konijnenberg A, Butterer A and Sobott F (2013) Native ion mobility-mass spectrometry and related methods in structural biology. *Biochimica et Biophysica Acta, Proteins and Proteomics* **1834**, 1239–1256.
- Kwon J, Lee Y, Lee T and Ahn J-H (2020) Aptamer-based field-effect transistor for detection of avian influenza virus in chicken serum. *Analytical Chemistry* **92**, 5524–5531.
- Kypr J, Kejnovská I, Renčíuk D and Vorlíčková M (2009) Circular dichroism and conformational polymorphism of DNA. *Nucleic Acids Research* **37**, 1713–1725.

- Largy E, König A, Ghosh A, Ghosh D, Benabou S, Rosu F and Gabelica V (2022) Mass spectrometry of nucleic acid noncovalent complexes. *Chemical Reviews* **122**, 7720–7839.
- Lau PS and Li Y (2014) Exploration of structure-switching in the design of aptamer biosensors. In Gu MB and Kim H-S (eds), *Biosensors Based on Aptamers and Enzymes*. Berlin: Springer, pp. 69–92.
- Le MT, Brown RE, Simon AE and Dayie TK (2015) *In vivo*, large-scale preparation of uniformly ¹⁵N- and site-specifically ¹³C-labeled homogeneous, recombinant RNA for NMR studies. *Methods in Enzymology* **565**, 495–535.
- Li JJ, Fang X and Tan W (2002) Molecular aptamer beacons for real-time protein recognition. *Biochemical and Biophysical Research Communications* **292**, 31–40.
- Li W, Yang X, Wang K, Tan W, Li H and Ma C (2008) FRET-based aptamer probe for rapid angiogenin detection. *Talanta* **75**, 770–774.
- Liao D, Jiao H, Wang B, Lin Q and Yu C (2012) KF polymerase-based fluorescence aptasensor for the label-free adenosine detection. *Analyst* **137**, 978–982.
- Lin CH and Patel DJ (1997) Structural basis of DNA folding and recognition in an AMP-DNA aptamer complex: Distinct architectures but common recognition motifs for DNA and RNA aptamers complexed to AMP. *Chemistry & Biology* **4**, 817–832.
- Lin P-H, Chen R-H, Lee C-H, Chang Y, Chen C-S and Chen W-Y (2011) Studies of the binding mechanism between aptamers and thrombin by circular dichroism, surface plasmon resonance and isothermal titration calorimetry. *Colloids and Surfaces, B: Biointerfaces*, **B 88**, 552–558.
- Lin P-H, Yen S-L, Lin M-S, Chang Y, Louis SR, Higuchi A and Chen W-Y (2008) Microcalorimetric studies of the thermodynamics and binding mechanism between L-tyrosinamide and aptamer. *Journal of Physical Chemistry B* **2008**, 6665–6673.
- Lipfert J, Das R, Chu VB, Kudaravalli M, Boyd N, Herschlag D and Doniach S (2007) Structural transitions and thermodynamics of a glycine-dependent riboswitch from vibrio cholerae. *Journal of Molecular Biology* **365**, 1393–1406.
- Liu X, Hou Y, Chen S and Liu J (2021) Controlling dopamine binding by the new aptamer for a FRET-based biosensor. *Biosensors & Bioelectronics* **173**, 112798.
- Liu X, Shi L, Hua X, Huang Y, Su S, Fan Q, Wang L and Huang W (2014) Target-induced conjunction of split aptamer fragments and assembly with a water-soluble conjugated polymer for improved protein detection. *ACS Applied Materials & Interfaces* **6**, 3406–3412.
- Lu C, Jimmy Huang P-J, Zheng J and Liu J (2022) 2-Aminopurine fluorescence spectroscopy for probing a glucose binding aptamer. *Chembiochem* **23**, e202200127.
- Lyklema J (ed.) (2000) *Fundamentals of Interface and Colloid Science*. London: Academic Press.
- Ma X, Qiao S, Sun H, Su R, Sun C and Zhang M (2019) Development of structure-switching aptamers for kanamycin detection based on fluorescence resonance energy transfer. *Frontiers in Chemistry* **7**, 29.
- Mehennaoui S, Poorahong S, Jimenez GC and Siaj M (2019) Selection of high affinity aptamer–ligand for dexamethasone and its electrochemical biosensor. *Scientific Reports* **9**, 6600.
- Mergny J-L and Lacroix L (2003) Analysis of thermal melting curves. *Oligonucleotides* **13**, 515–537.
- Morris FD, Peterson EM, Heemstra JM and Harris JM (2018) Single-molecule kinetic investigation of cocaine-dependent split-aptamer assembly. *Analytical Chemistry* **90**, 12964–12970.
- Morse DP (2007) Direct selection of RNA beacon aptamers. *Biochemical and Biophysical Research Communications* **359**, 94–101.
- Nakatsuka N, Yang K-A, Abendroth JM, Cheung KM, Xu X, Yang H, Zhao C, Zhu B, Rim YS, Yang Y, Weiss PS, Stojanović MN and Andrews AM (2018) Aptamer-field-effect transistors overcome Debye length limitations for small-molecule sensing. *Science* **362**, 319–324.
- Neves MD, Reinstein O and Johnson PE (2010) Defining a stem length-dependent binding mechanism for the cocaine-binding aptamer. A combined NMR and calorimetry study. *Biochemistry* **49**, 8478–8487.
- Neves MD, Shoara AA, Reinstein O, Abbasi Borhani O, Martin TR and Johnson PE (2017) Optimizing stem length to improve ligand selectivity in a structure-switching cocaine-binding aptamer. *ACS Sensors* **2**, 1539–1545.
- Nutiu R and Li Y (2003) Structure-switching signaling aptamers. *Journal of the American Chemical Society* **125**, 4771–4778.
- Nutiu R and Li Y (2005) *In vitro* selection of structure-switching signaling aptamers. *Angewandte Chemie, International Edition* **44**, 1061–1065.
- Oguro A, Yanagida A, Fujieda Y, Amano R, Otsu M, Sakamoto T, Kawai G and Matsufuji S (2017) Two stems with different characteristics and an internal loop in an RNA aptamer contribute to spermine-binding. *Journal of Biochemistry* **161**, 197–206.
- Oh SS, Plakos K, Lou X, Xiao Y and Soh HT (2010) *In vitro* selection of structure-switching, self-reporting aptamers. *Proceedings of the National Academy of Sciences of the United States of America* **107**, 14053–14058.
- Perez-Gonzalez C, Lafontaine DA and Penedo JC (2016) Fluorescence-based strategies to investigate the structure and dynamics of aptamer–ligand complexes. *Frontiers in Chemistry* **4**, 33.
- Qiao Q, Guo X, Wen F, Chen L, Xu Q, Zheng N, Cheng J, Xue X and Wang J (2021) Aptamer-based fluorescence quenching approach for detection of aflatoxin M1 in milk. *Frontiers in Chemistry* **9**, 653869.
- Reinstein O, Neves MD, Saad M, Boodram SN, Lombardo S, Beckham SA, Brouwer J, Audette GF, Groves P, Wilce MCJ and Johnson PE (2011) Engineering a structure switching mechanism into a steroid binding aptamer and hydrodynamic analysis of the ligand binding mechanism. *Biochemistry* **50**, 9368–9376.
- Reinstein O, Yoo M, Han C, Palmo T, Beckham SA, Wilce MCJ and Johnson PE (2013) Quinine binding by the cocaine-binding aptamer. Thermodynamic and hydrodynamic analysis of high-affinity binding of an off-target ligand. *Biochemistry* **52**, 8652–8662.
- Robertson SA, Harada K, Frankel AD and Wemmer DE (2000) Structure determination and binding kinetics of a DNA aptamer–argininamide complex. *Biochemistry* **39**, 946–954.
- Sakamoto T (2017) NMR study of aptamers. *Aptamers* **1**, 13–18.
- Schmidt C, Perbandt M, Klusmann S and Betzel C (2020) Molecular characterization of a ghrelin-l-aptamer complex. *Journal of Molecular Structure* **1204**, 127510.
- Slavkovic S and Johnson PE (2018) Isothermal titration calorimetry studies of aptamer-small molecule interactions: Practicalities and pitfalls. *Aptamers* **2**, 45–51.
- Slavkovic S and Johnson PE (2023) Analysis of aptamer-small molecule binding interactions using isothermal titration calorimetry. In Mayer G and Menger MM (eds), *Nucleic Acid Aptamers: Selection, Characterization, and Application*. New York: Springer US, pp. 105–118.
- Sokoloski JE, Dombrowski SE and Bevilacqua PC (2012) Thermodynamics of ligand binding to a heterogeneous RNA population in the malachite green aptamer. *Biochemistry* **51**, 565–572.
- Spolar RS and Record M, Jr (1994) Coupling of local folding to site-specific binding of proteins to DNA. *Science* **263**, 777–784.
- Stojanovic MN, De Prada P and Landry DW (2000) Fluorescent sensors based on aptamer self-assembly. *Journal of the American Chemical Society* **122**, 11547–11548.
- Tuleuova N, Jones CN, Yan J, Ramanculov E, Yokobayashi Y and Revzin A (2010) Development of an aptamer beacon for detection of interferon-gamma. *Analytical Chemistry* **82**, 1851–1857.
- Ueyama H, Takagi M and Takenaka S (2002) A novel potassium sensing in aqueous media with a synthetic oligonucleotide derivative. Fluorescence resonance energy transfer associated with guanine quartet–potassium ion complex formation. *Journal of the American Chemical Society* **124**, 14286–14287.
- Velázquez-Campoy A, Ohtaka H, Nezami A, Muzammil S and Freire E (2004) Isothermal titration calorimetry. *Current Protocols in Cell Biology* **23**, 17.18.11–17.18.24.
- Wang RE, Zhang Y, Cai J, Cai W and Gao T (2011) Aptamer-based fluorescent biosensors. *Current Medicinal Chemistry* **18**, 4175–4184.
- Wang X, Yu B, Sakurabayashi S, Paz-Villatoro JM and Iwahara J (2024) Robust enzymatic production of DNA G-quadruplex, aptamer, DNazyme, and other oligonucleotides: Applications for NMR. *Journal of the American Chemical Society* **146**, 1748–1752.
- Wang Z, Yu H, Canoura J, Liu Y, Alkhamis O, Fu F and Xiao Y (2018) Introducing structure-switching functionality into small-molecule-binding aptamers via nuclease-directed truncation. *Nucleic Acids Research* **46**, e81–e81.
- Weeks KM (2021) SHAPE directed discovery of new functions in large RNAs. *Accounts of Chemical Research* **54**, 2502–2517.

- Wu Y, Ranallo S, Del Grosso E, Chamoro-Garcia A, Ennis HL, Milosavić N, Yang K, Kippin T, Ricci F, Stojanovic M and Plaxco KW** (2023) Using spectroscopy to guide the adaptation of aptamers into electrochemical aptamer-based sensors. *Bioconjugate Chemistry* **34**, 124–132.
- Wüthrich K** (1986) *NMR of Proteins and Nucleic Acids*. New York: John Wiley & Sons.
- Xie Y, Wu S, Chen Z, Jiang J and Sun J** (2022) Rapid nanomolar detection of methamphetamine in biofluids via a reagentless electrochemical aptamer-based biosensor. *Analytica Chimica Acta* **1207**, 339742.
- Xu G, Wang C, Yu H, Li Y, Zhao Q, Zhou X, Li C and Liu M** (2023) Structural basis for high-affinity recognition of aflatoxin B1 by a DNA aptamer. *Nucleic Acids Research* **51**, 7666–7674.
- Xu G, Zhao J, Yu H, Wang C, Huang Y, Zhao Q, Zhou X, Li C and Liu M** (2022) Structural insights into the mechanism of high-affinity binding of ochratoxin a by a DNA aptamer. *Journal of the American Chemical Society* **144**, 7731–7740.
- Yang C, Wang Y, Marty J-L and Yang X** (2011) Aptamer-based colorimetric biosensing of ochratoxin a using unmodified gold nanoparticles indicator. *Biosensors & Bioelectronics* **26**, 2724–2727.
- Yang K-A, Pei R and Stojanovic MN** (2016) In vitro selection and amplification protocols for isolation of aptameric sensors for small molecules. *Methods* **106**, 58–65.
- Zhang Z, Oni O and Liu J** (2017) New insights into a classic aptamer: Binding sites, cooperativity and more sensitive adenosine detection. *Nucleic Acids Research* **45**, 7593–7601.
- Zimmer DP and Crothers DM** (1995) NMR of enzymatically synthesized uniformly $^{13}\text{C}^{15}\text{N}$ -labeled DNA oligonucleotides. *Proceedings of the National Academy of Sciences of the United States of America* **92**, 3091–3095.